Journal of
Analytical & Bioanalytical Techniques

Szczygieł et al., J Anal Bioanal Tech 2014, 5:6
DOI: 10.4172/2155-9872.1000227

Research Article Open Access

Real-time Non-invasive Transdermal Monitoring of Photosensitizer Level *in vivo* for Pharmacokinetic Studies and Optimization of Photodynamic Therapy Protocol

Małgorzata Szczygieł[1*], Bożena Boroń[1,2], Dariusz Szczygieł[1], Milena Szafraniec[1], Anna Susz[1], Zenon Matuszak[3], Krystyna Urbanska[1] and Leszek Fiedor[1*]

[1]*Faculty of Biochemistry, Biophysics and Biotechnology, Jagiellonian University, Kraków, Poland*
[2]*Institute of Physics, University of Silesia, Katowice, Poland*
[3]*Department of Biophysics and Medical Physics, Faculty of Physics and Computer Science, AGH University of Science and Technology, Kraków, Poland*

Abstract

Efficient application of any therapeutic agent requires the knowledge of the time evolution of drug concentration in tissues. Usually, the collection of such pharmacokinetic data relies on sequential invasive measurements and sacrifice of many animals. Our aim was to establish a non-invasive analytical assay that would allow for determination of the levels of fluorescent (pro)drugs in the tissues. We have applied a portable fiber optics-based spectrophotometric setup to determine pharmacokinetic profiles of two water-soluble chlorophyll derivatives via transdermal emission measurements in vivo, in a model system consisting of DBA/2 mice bearing subcutaneous Cloudman S91 melanoma tumor. Based on their emission spectra, recorded transdermally in real-time, the in vivo peak levels and retention times of intraperitoneally and intravenously administered photosensitizers were estimated. These data served then to optimize the photodynamic therapy protocol. The effects of the treatment show a strong correlation between the efficacy of the therapy and the pharmacokinetic profiles, confirming the validity of the method. This approach has several important advantages, including (i) a maximization of therapeutic effects by indicating the optimal timing for irradiation; (ii) a non-invasive determination of the photosensitizer level in the tumor to predict the therapy outcome; (iii) an estimation of the safety dark period to minimize the side effects related to phototoxicity; (iv) a possibility of performing a whole series of non-invasive pharmacokinetic experiments in the same organism; and (v) a significant cut in the costs of pharmacokinetic studies. The measurements on human tissue indicate that this non-invasive method can be also applied in humans.

Keywords: Photosensitizer; Miniature spectrophotometer; Fiber optics; *in vivo* emission detection; Chlorophyllides; Therapeutic window

Abbreviations: (B)Chl: (bacterio)chlorophyll; Chlide: chlorophyllide a; i.p.: intraperitoneally; i.v.: intravenously; MTT: 3-(4,5-dimethylthiazol-2-yl)-2,5-diphenyl tetrazolium bromide; PBS: phosphate-buffered saline; PDT: photodynamic therapy; Zn-Pheide: Zn-pheophorbide a

Introduction

Accurate information about the actual drug concentration in tissues is obviously critical to any therapy but unfortunately it is not always available. The effective application of a drug, to achieve its maximal impact on target tissues with minimal side effects, relies on knowledge of the changes in drug levels in tissues [1,2]. In practice, to collect such pharmacokinetic data an invasive and tedious monitoring of administered drug is needed, meaning the continual sacrifice of a large number of experimental animals. This procedure necessarily increases the costs of evaluating drugs and raises ethical problems, so there is a need for non-invasive imaging of the distribution and retention of drugs in living organisms [3,4]. This is true in particular of aggressive drugs used, for instance, in chemotherapy, or the application of pro-drugs, such as light-activated photosensitizers in photodynamic therapy (PDT). It is only the recent development of fiber optic technology paralleled by advances in fiber optic based spectrometers that bring us closer to this goal. This technological progress increases the significance of various kinds of phototherapies in which very localized and precise light delivery is required, and also opens new directions for applications in diagnostics. The use of flexible fiber optics allows one to perform measurements in ways that conventional spectroscopic methods cannot be applied, such as handheld imaging or imaging in living organisms without sedation [1,5-8]. *In vivo* fluorometry is one such non-invasive method for the determination of the pharmacokinetic profiles of fluorescent photosensitizers, which might be helpful in selecting the appropriate parameters for effective PDT [1,9]. What is more, by the use of fiber optics, the fluorophore can be excited in the very proximity of the fiber tip, thus allowing for *in situ* determination of its concentration [10].

Chlorophylls (Chls) and bacteriochlorophylls (BChls), the major photosynthetic pigments, have many benefits of excellent photosensitizers, including high yields of triplet states and very intensive light absorption in the near-infrared region of the spectrum, which coincides with the therapeutic window of human tissue [11-14]. Moreover, if not substituted with transition metal ions, they remain

***Corresponding author:** Professor Leszek Fiedor, Faculty of Biochemistry, Biophysics & Biotechnology, Jagiellonian University, 7 Gronostajowa Street, Kraków 30-387, Poland, Tel: ++48-12-6646358; Fax: ++48-12-6646902; E-mail: leszek.fiedor@uj.edu.pl

Dr. Małgorzata Szczygieł, Faculty of Biochemistry, Biophysics & Biotechnology, Jagiellonian University, 7 Gronostajowa Street, Kraków 30-387, Poland, Tel: ++48-12-664 64 30; Fax: ++48-12-664 69 02; E-mail: gosia.szczygiel@uj.edu.pl

Received October 24, 2014; **Accepted** November 29, 2014; **Published** December 3, 2014

Citation: Szczygieł M, Boroń B, Szczygieł D, Szafraniec M, Susz A, et al. (2014) Real-time Non-invasive Transdermal Monitoring of Photosensitizer Level in vivo for Pharmacokinetic Studies and Optimization of Photodynamic Therapy Protocol. J Anal Bioanal Tech 5: 227 doi:10.4172/2155-9872.1000227

fluorescent which makes them promising as markers for *in vivo* and *in vitro* detection [14]. The main aim of the present study was to evaluate the usefulness of *in vivo* fluorometry in establishing an assay for the non-invasive determination of the pharmacokinetic profiles of Chl-derived photosensitizers and applying them to maximize the efficacy of Chl-based PDT. To this end, direct trans-dermal *in vivo* monitoring of fluorescent Chl-derived photosensitizers via fluorescence detection was carried out in mice with S91 melanoma, using a fiber optic probe and a miniaturized diode array spectrometer. The collected spectroscopic data enabled us to estimate the time needed to reach the peak concentration of a photosensitizer in a tumor after either intraperitoneal (i.p.) or intravenous (i.v.) administration. On this basis the optimal timing for light treatment was determined. We also show that this timing correlates well with the high efficacy of PDT in mice.

Materials and Methods

Chemicals

The solvents were either of analytical (POCh, Gliwice, Poland) or HPLC (Merck, Darmstadt, Germany) grade. The phosphate-buffered saline (PBS), Roswell Park Memorial Institute medium (RPMI) and antibiotics for cell culture were purchased from Biomed, Lublin, Poland. 3-(4,5-dimethylthiazol-2-yl)-2,5-diphenyl tetrazolium bromide (MTT) and Cremophore® were from Sigma Chemical Co. (Steinheim, Germany).

Photosensitizers

Chlorophyll a (Chla) was extracted from fresh spinach leaves and purified following a published procedure [15]. Chlorophyllide a (Chlide) was obtained by hydrolysis of Chla using a plant enzyme chlorophyllase overexpressed in *E. coli* [16]. The product was purified by column chromatography on CM-Sepharose CL-6B (Pharmacia) as described previously [15]. Pheophorbide a (Pheide) was obtained from Chlide by demetalation via a short treatment with glacial acetic acid. After completion of the reaction, as monitored spectrophotometrically and by TLC, the acid was removed in a stream of nitrogen and the product purified by column chromatography on CM-Sepharose CL-6B, as described above. Zn-substituted Chlide (Zn–Pheide) was obtained from Pheide via direct metalation with zinc acetate in methanol [17]. Zn–Pheide was purified twice by column chromatography on CM-Sepharose CL-6B, as above. All pigments, after thorough drying under vacuum, were stored at −30°C under Ar. The preparatory steps were performed as quickly as possible in dim light to avoid pigment degradation. The purity of the photosensitizers was confirmed spectrophotometrically on a Cary 400 spectrophotometer (Varian, USA) and by HPLC on a reversed-phase silica gel column [13].

Cell line

Cloudman S91 mouse melanoma cells subline S91/I3 came from the laboratory of Dr. Pawelek (Yale School of Medicine, New Haven CT, USA). The cells were grown as a monolayer in plastic cell culture flasks in an RPMI 1640 medium supplemented with 100 units/ml of penicillin, 100 μg/ml streptomycin and 5% fetal calf serum (Gibco, Grand Island NY, USA). Cells were cultivated in Petri dishes and incubated at 37°C in a humid atmosphere containing 5% CO_2.

In vitro photosensitizer uptake

The S91 cells were seeded on 6-well plates (1×10^5 cells per well) and incubated overnight (37°C, 5% CO_2). Then the cells were treated with solutions containing various concentrations of Chlide or Zn–Pheide (from 10 to 400 nM) in 2 ml culture medium. After 3 h of incubation with the photosensitizer, the cells were rinsed with 1 ml of PBS, spun down and suspended in 0.5 ml of acetone. The intensity of the fluorescence from these cell extracts, upon excitation at 410 nm (the Soret band), served to estimate the quantities of photosensitizers accumulated in the cells. In parallel, fluorescence measurements were done directly on the cells growing on the 96-well cell plates (1×10^4 cells per well). The S91 cells were incubated with solutions of Chlide or Zn–Pheide (5 h of incubation with concentrations varying from 250 to 2500 nM, or an incubation period varying from 0.5 h to 5 h at 2500 nM), then the photosensitizer solution was removed from the plate, the cells were rinsed with PBS and the emission of the photosensitizer accumulated inside the cells was measured on a Tecan reader using excitation at 410 nm.

Animals

The male DBA/2 mice used in the experiments were 3-8 months old and of 20-28 g in weight. They came from the animal house of the Mossakowski Medical Research Center, Polish Academy of Science in Warsaw, Poland. The animals underwent two weeks of acclimatization in the local animal house before the experiments were carried out. They were kept in a 12 h light/dark day cycle and were fed on standard laboratory chew for rodents (LaboFeed B from Morawski, Kcynia, Poland) with free access to fresh water. All experiments on animals were approved by the First Local Ethics Committee for Experiments on Animals at the Jagiellonian University in Cracow (permissions No. 13/2010 and 132/2010).

Tumor implantation

The S91 cells, about 0.5×10^6 in number, were suspended in 50 μl of PBS (with Ca^{2+} and Mg^{2+} ions) and implanted intradermally into the right thighs of mice. The skin surrounding the injection site was shaved with a razor before the implantation. During the shaving and tumor implantation the animals were held still for about 30 s. The tumors emerged in about 10 days after implantation. Their mean diameters were estimated using the formula $d=\sqrt[3]{a\cdot b\cdot c}$, where a, b and c are three perpendicular diameters measured using a caliper [13]. When the d value reached about 3-5 mm, the animal was considered ready for treatment. To determine the kinetics of tumor growth their volumes were estimated according to the formula $v=\frac{\pi}{6}(a\cdot b\cdot c)$.

Administration of photosensitizers

In all experiments, 44 tumor bearing mice divided into two experimental subgroups, one treated with Chlide and the other one with Zn–Pheide, were used. The photosensitizer solutions were freshly prepared before administration. Two types of administration were used, i.v. (through the tail vein) and i.p. To prepare the solutions for injection, portions of the pigments at a dose of either 2 mg (i.v.) or 10 mg (i.p.) per 1 kg of animal body weight, were dissolved in a small volume of ethanol and 100 μl (or 500 μl for the i.p.) of water containing PBS (9:1, v/v), then sonicated for three minutes and spun down (2000 g, 8 min, room temperature) to remove solid residue. Supernatants were administered to the animals immediately after centrifugation.

In another experiment, to increase bioavailability, the pigments in the i.v. protocol were administered using a non-ionic surfactant Cremophore®. Their solutions were prepared as described above and Cremophore® (2 mg/kg of animal weight) was added to the solution prior to centrifugation. The experimental conditions applied in the present study are summarized in Table 1 and the flow chart of the

entire experiment is shown in Scheme 1.

In vivo fluorescence measurements

The measurements were performed using a portable USB2000 spectrometer (Ocean Optics, USA) based on a 2048-element linear silicon CCD array and equipped with a QR200-7-UV-Vis Fiber Fluorescence Probe (Ocean Optics, USA). The probe consisted of 6 illumination silica fibers (200 μm ± 4 μm in diameter) surrounding one read silica fiber (200 μm ± 4 μm in diameter) situated in the center of stainless steel ferrule. The construction of the fluorescence probe was such as to eliminate any back reflection from the excitation beam, resulting in a higher signal than that achieved with a traditional configuration. The measurements were performed with non-contact illumination and detection. The probe was always positioned in such a way with respect to the skin surface that the fluorescence amplitude was maximal. For the excitation of the photosensitizer accumulated inside the tumor an LS-450 Blue LED light source (Ocean Optics, USA) emitting at 380 nm was used. The emission spectra were collected using OOIBase32 operating software. The background level was recorded prior to photosensitizer administration in the same manner. The fluorescence signal from the tissue was recorded 3 times with an integration time of 80 ms and then averaged.

Monitoring of photosensitizer level in tumors *in vivo*

The administered photosensitizer was excited directly through the skin of the animal using the LS-450 light source. The fluorescence was measured 15 minutes after drug administration and then in 15-30 min intervals until the signal started to decline. Immediately afterwards the tumor was irradiated according to the PDT protocol.

Irradiation protocol

A diode laser emitting at 655 nm (beam diameter 1 cm, power density 60 mW/cm^2) equipped with a moveable head (Creotech, Poland) was used to irradiate the tumors. The total light dose delivered to the tumor during 25 min of irradiation was 100 J/cm^2.

Statistics

The pharmacokinetics of the photosensitizers in tumors was evaluated after the administration of Chlide to 19 mice (i.p. N=5; i.v. N=8; i.v., with the surfactant, N=6) and Zn–Pheide to 20 mice (i.p. N=7; i.v. N=8; i.v., with the surfactant, N=5). The response of tumors to PDT with Zn–Pheide was analyzed in 21 mice, subjected to four different therapeutic protocols (i.p., irradiation after 3-4 h, N=5; i.v., irradiation after 3-4 h, N=7; i.v., with the surfactant, irradiation after 0.5 h or 3-4 h, N=4 and N=5, respectively). The analysis of the tumor response to PDT depending on the intensity of photosensitizer fluorescence in the tumor (low or high intensity) measured just before irradiation, was performed on 15 mice treated with Chlide (irradiation after 1.5-3 h; i.p. N=4; i.v. N=6; i.v., with surfactant, N=5) and 17 mice treated with Zn–Pheide (irradiation after 3-4 h; i.p. N=5; i.v. N=7; i.v., with the surfactant, N=5). The control group consisted of 12 mice bearing tumors which were irradiated but were not given the photosensitizer. All results are presented as the means ± SE.

Results

Photosensitizer uptake by tumor cells *in vitro*

The uptake of Chlide and Zn–Pheide by S91 tumor cells was assayed both in the cell extracts and directly in the cells. In both cases, the intensity of photosensitizer fluorescence, measured directly in the cells, was approximately proportional to its concentration in the incubation medium and, typically, the signal from Chlide was about two times stronger than that from Zn–Pheide (Figure 1B). The estimation of photosensitizer content in S91 cells based on the extraction also showed a linear correlation of photosensitizer accumulation in the cells with the pigment dose (Figure 1A). The concentration of pigments in the cells after e.g. 3.5 h incubation time was about 20-30 times higher than in the incubation medium (Figure 1A), in agreement with our previous study [14]. As expected, the increase of incubation time from 0.5 to 5 h leads to a higher accumulation of photosensitizers in cells (13 fold and 8 fold, respectively) (Figure 1C). The direct assay showed that during that time the saturation of cells was not reached (Figure 1C).

In vivo monitoring of photosensitizer level in tumor

In order to eliminate the distortion of blood flow in the tissue induced by pressing of the probe against the skin, and to eliminate the scattering of light from the skin surface measurements were performed in a non-contact mode [1,18,19]. Because the animals were not sedated during the experiment the measurements could not be performed in complete darkness. After administration (i.p. or i.v.) of the photosensitizers into the tumor bearing mice a characteristic fluorescence signal was already detectable in the tumors upon the first measurement, i.e. after 15-20 minutes (Figures 2A & 2B). The emission spectra from each tumor were recorded at 15-30 min intervals. In the range of 650 nm to 700 nm no emission from endogenous fluorophores was observed whereas the maximum of the Chlide fluorescence band was located at 674 nm and that of Zn–Pheide at 670 nm (Figure 2A). As shown in Figure 2B, the intensity of the characteristic emission signal grows to reach a maximum and then it declines, obviously reflecting the kinetics of photosensitizer accumulation and then clearance from the tumor.

The same conditions were applied to measure the emission spectra of human skin under dim light and in the dark, in the absence of photosensitizer (Figure 2C). As in the animal skin, the spectrum

Photosensitizer	Administration dose per kg, carrier	No. of animals	*In vivo* emission peak time [h]	Irradiation lag [h]	Photosensitizer level in tumor	Tumor response to PDT
Zn–Pheide	i.v. 2 mg, PBS+Cremophore®	4	0.62	0.5	high	high
	i.v. 2 mg, PBS+Cremophore®	5	0.62	3 – 4	medium	medium
	i.v. 2 mg, PBS	7	1.95	3 – 4	low	low
	i.p. 10 mg, PBS	5	3.28	3 – 4	high	high
Chlide	i.v. 2 mg, PBS+Cremophore®	5	0.80	1.5 – 3	high	medium
	i.v. 2 mg, PBS	6	0.79	1.5 – 3	medium	low
	i.p. 10 mg, PBS	4	1.44	1.5 – 3	high	medium
Control	PBS	12	–	0.5 – 3	–	–

Table 1: Experimental conditions and outcome of various PDT protocols based on the *in vivo* monitoring of photosensitizer level in tumor (see the text for details).

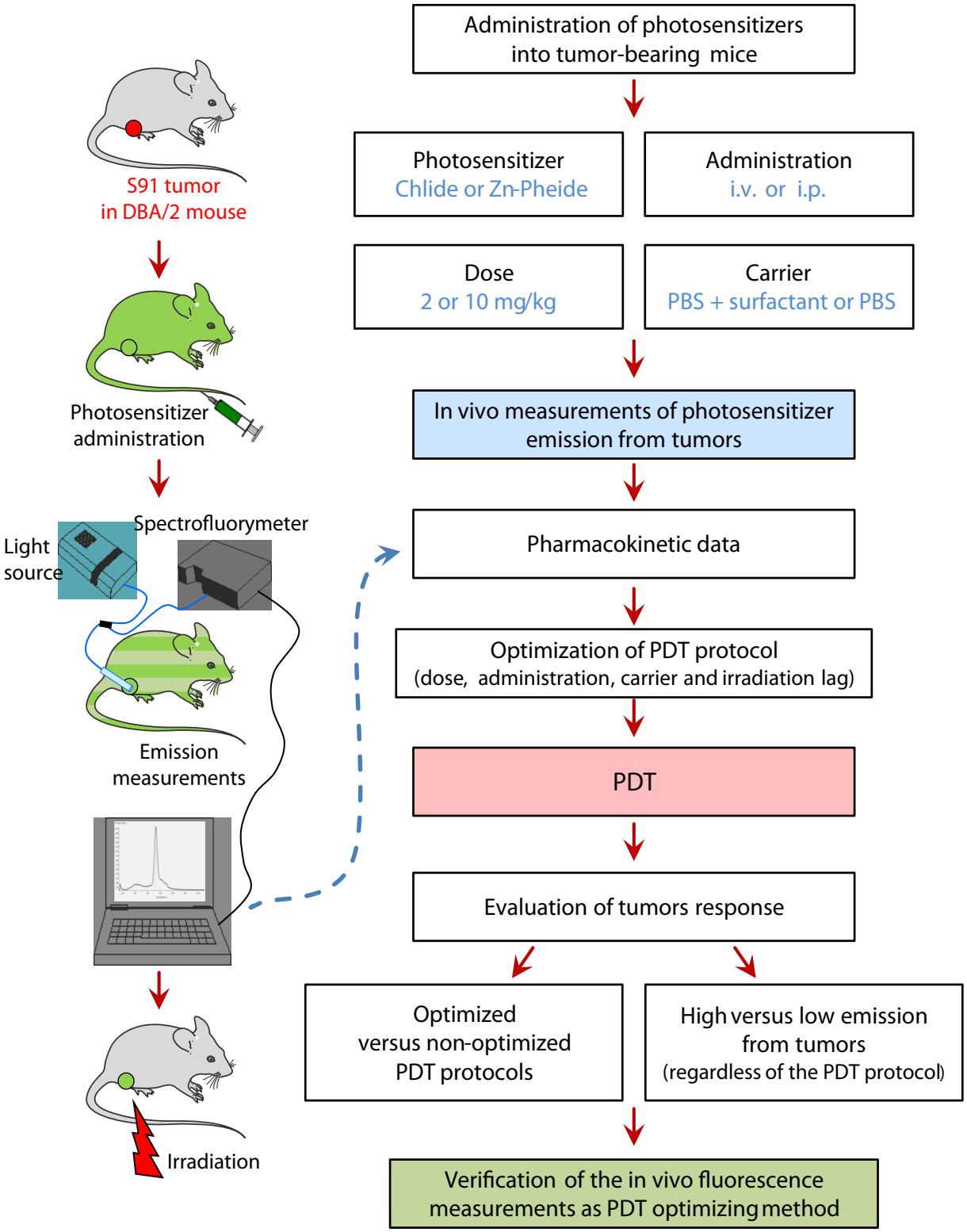

Scheme 1: The outline of the experimental setup and conditions applied in optimization of PDT in mice, based on the non-invasive monitoring of photosensitizer level *in vivo*.

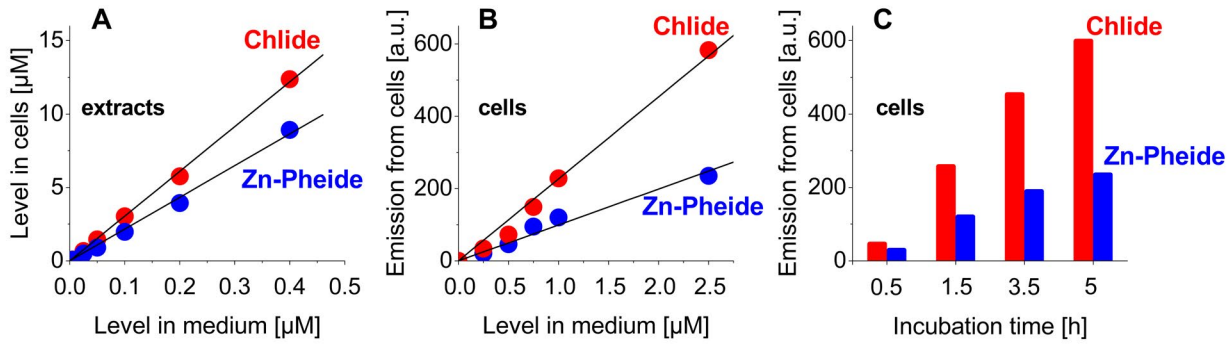

Figure 1: Photosensitizer uptake by S91 melanoma cells *in vitro*. (A) The accumulation of the photosensitizers estimated fluorometrically from acetone cell extracts. (B) Dependence of photosensitizer emission intensity on its concentration in the incubation medium measured directly in tumor cells. (C) Kinetics of photosensitizer cellular uptake measured fluorometrically directly from tumor cells grown *in vitro* using Tecan reader (see the text for details).

recorded under dim day light shows bands due to stray light and the second harmonic component. The spectrum recorded in the dark shows only the second harmonic band.

The examination of two experimental groups treated with either Chlide or Zn–Pheide provided data to determine the pharmacokinetic profiles of the two photosensitizers (Figure 3). The peak level of Zn–Pheide in the tumors was reached after a significantly longer period than that of Chlide, independently of the administration protocol. However, with both Chlide and Zn–Pheide, the maximum of the emission was observed 1-2 hours earlier after i.v. administration, and the signal from the latter pigment was significantly lower. After i.p. administration, similar amplitudes of Zn–Pheide and Chlide emissions were observed (Figure 3).

When a non-ionic surfactant Cremophore® was used to solubilize the pigments for i.v. administration, a 2-3 fold increase in the fluorescence amplitude in the tumor was seen along with a shortening of the time required to reach the maximal emission from Zn–Pheide (Figure 3). In consequence, the peak time of Zn–Pheide matched that of Chlide (either with or without the surfactant).

The emission signals from the i.p. administered Zn–Pheide at 10 mg/kg were 3-fold higher than those recorded after i.v. administration at a dose of 2 mg/kg. However, i.v. administration Zn–Pheide in the surfactant yielded the maximum emission signal in the tumors of the same level as after its i.p. administration at the 5-fold higher dose. In addition, the maximal signals from ZnPheide appear at quite different times after i.v. (with the surfactant) and i.p. administrations, i.e. after 0.5 h and 3.5 h, respectively (Figure 3). In tumors of similar size, i.v. administration of a better soluble Chlide (2 mg/kg) resulted in similar fluorescence intensity as in the case of the i.p. route at 10 mg/kg. The use of the surfactant to administer Chlide i.v. (2 mg/kg) yielded a maximum signal approximately 2-fold higher than after its i.p. administration at a much higher dose (10 mg/kg). Similarly, the two ways of administration yielded a peak signal of Chlide emission from the tumors after significantly different periods, 45 min and 90 min, respectively (Figure 3).

Optimization of PDT protocol

The times after which the two photosensitizers, administered in various ways, reach their maximal levels in tumor tissue are compared in Figure 4. The optimal time window for Zn–Pheide opens 190 minutes after i.p. injection and 120 minutes after i.v. administration, and after as short as 40 minutes when the surfactant was applied. The corresponding timings for Chlide are 90, 45 and 45 min, respectively. The optimization of the PDT protocol was done using Zn–Pheide due to its relatively wide optimal time window. The extended duration of the time window in the case of Zn-Pheide is in line with its pharmacokinetic profile and its high efficacy against the A549 tumors in mice [13,14].

The steps taken to achieve optimization of the PDT protocol based on the *in vivo* monitoring of photosensitizer level are outlined in Scheme 1 and Table 1 summarizes the conditions and outcomes of the protocols applied. The PDT on the S91 tumor was performed according to four different protocols with the irradiation timing selected in line with the pharmacokinetic data (Figure 4): (i) Zn–Pheide (2 mg/kg) in the surfactant with 20 min irradiation lag; (ii) Zn–Pheide (2 mg/kg) in the surfactant with 3-4 h irradiation lag; (iii) Zn–Pheide (2 mg/kg) without the surfactant with 3-4 h irradiation lag; (iv) Zn–Pheide (10 mg/kg) without the surfactant and with 3-4 h irradiation lag. The results of the treatments are presented as the kinetics of tumor growth in Figure 5. The strongest tumor response was observed in scheme (i), apparently because of the highest level of Zn–Pheide in the tumors. Clearly weaker effects were seen in scheme (ii), where the irradiation was applied after the photosensitizer had partially cleared from the tumor. Protocol (iii) gave the poorest results, seemingly because the Zn–Pheide level was too low in tumors, as achieved without the use of the surfactant). The responses to PDT in the animals treated with optimized schemes (i) and (iv) were similar (i.e. very strong inhibition of tumor growth), although the former protocol produced a slightly better effect (Figure 5). The monitoring of tumor growth after the treatment in the groups of animals with low and high level of photosensitizer emission, recorded prior to irradiation, show a greater response in the latter case (Figure 6).

Discussion

The objective of this study was to verify whether transdermal *in vivo* fluorescence measurements can be applied to optimize the photodynamic therapy of cancer. This involved a determination of the effects of the optimal dose, the carrier, the route of administration and the irradiation time. The study also addressed whether *in vivo* measurement of the photosensitizer fluorescence in the tumor just before irradiation may be regarded as a prognostic factor in the photodynamic therapy of cancer.

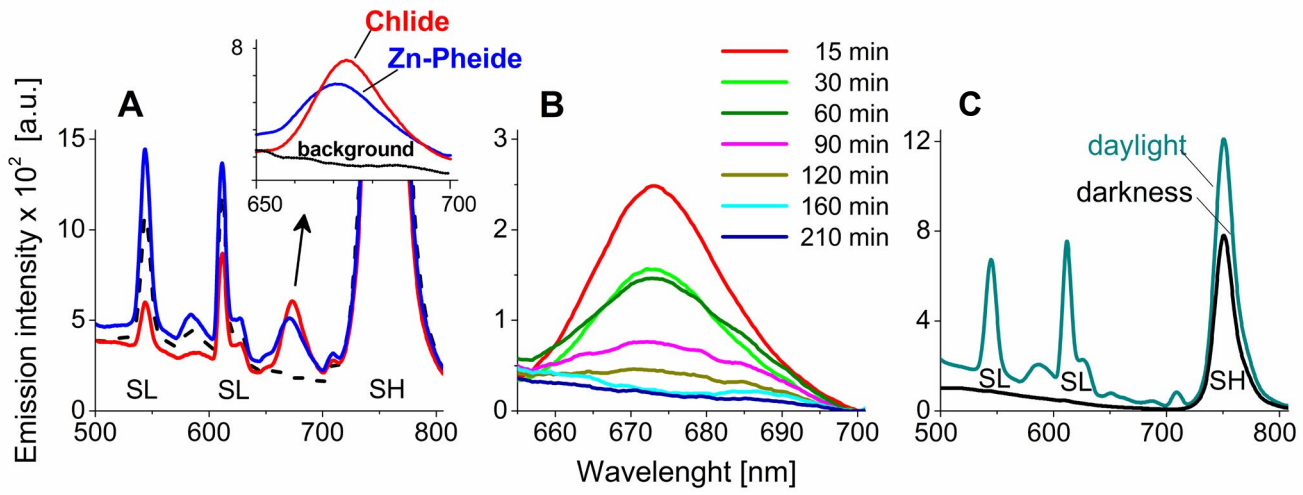

Figure 2: The emission spectra of tumors after administration of Chlide and Zn–Pheide, recorded in real-time mode. (A) Fluorescence spectra recorded *in vivo* from tumors after the Chlide, Zn–Pheide or carrier alone (PBS, water and ethanol) administration. In the inset the expanded region 650-700 nm is shown. (B) The emission spectra of the highest amplitude, selected from a series of measurements recorded for each time point. The spectra were recorded *in vivo* from a single tumor at various time intervals after Chlide administration (i.v., 2 mg/kg). (C) The emission spectra of human skin measured after excitation at 380 nm in daylight and in the darkness (see the text for details). SL - stray light, SH - second harmonic.

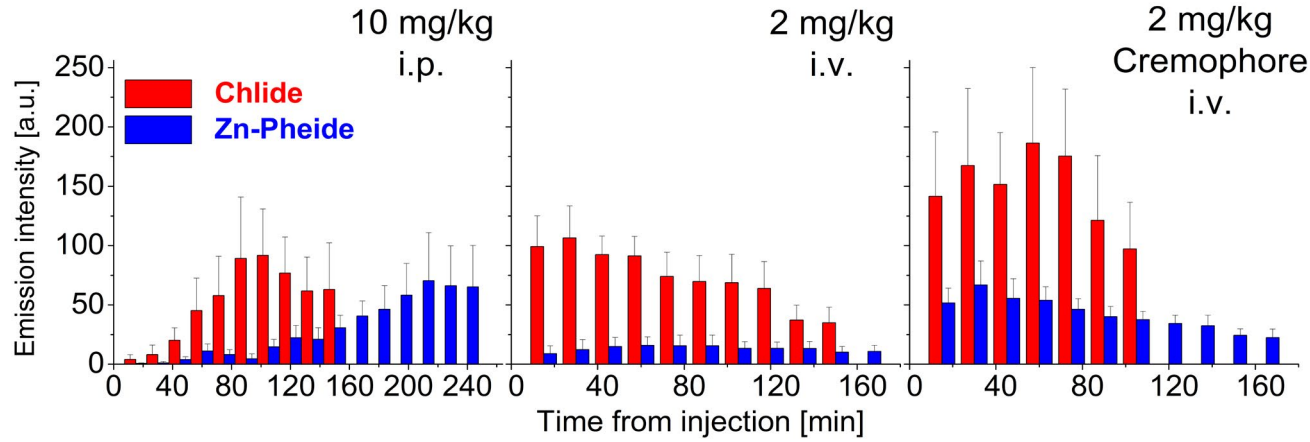

Figure 3: Pharmacokinetic profiles of Chlide and Zn–Pheide in S91 melanoma tumors estimated from the *in vivo* emission measurements shown in Figure 2. The profiles were determined for different doses of photosensitizers and ways of their administration as indicated (see the text for details). The results are shown as mean with SE.

Photosensitizer uptake by tumor cells *in vitro*

Both the direct fluorescence measurements in S91 cells growing on culture plates using a Tecan reader and spectrofluorometric measurements of acetone extracts from cells demonstrate that significant amounts of photosensitizers can accumulate in tumor cells. Their accumulation increases with concentration and incubation time. This shows that the cellular uptake of the pigments is diffusion-driven, as in our previous study [14]. At the highest applied dose (2.5 μM) the accumulation in the S91 cells did not reach the saturation level. The capacity of the S91 cell line to accumulate Zn–Pheide seems to be relatively high compared to the other lines (A549, MCF-7, LoVo) [14]. Even at a concentration of only 100 nM the signal from the former is high, while from the latter it is at background level.

In vivo monitoring of photosensitizer level in tumor

The measurements conducted on S91 tumors in the visible range showed the presence of several emission bands due to daylight. The intense band at 750 nm (Figure 2A) is a second harmonic line of the excitation light generated in the skin [20,21]. None of these additional bands overlaps with the fluorescence maxima of the photosensitizers used. The similarity of the emission spectra of human and animal skin (Figures 2A and 2C) indicates their similar spectral properties and shows the applicability of this approach in humans. Moreover, if the measurement is done in darkness, the drugs emitting in other spectral areas can be detected using this technique (Figure 2C). The emission signals of the highest amplitude were chosen as representative for the estimation of the photosensitizer level in tumor. A preliminary study on mice with advanced S91 tumors administered Chlide indicated that the signal kinetics, estimated that way, parallel the kinetics of photosensitizer level in tumors as estimated in tissue extracts (not shown).

Characteristic emission signals appear in tumors during the first 60 min after the administration of photosensitizers. Their intensity

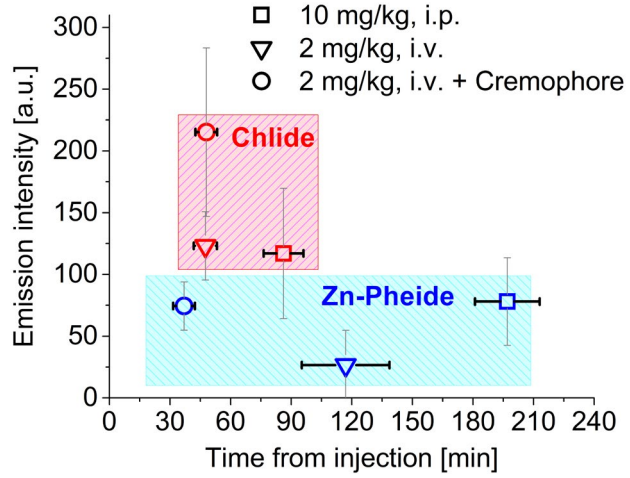

Figure 4: The optimal time windows for effective irradiation of S91 tumors treated with Chlide (red box) and Zn–Pheide (blue box) for different doses of photosensitizers and ways of their administration (see the text for details). The results are shown as means with SE.

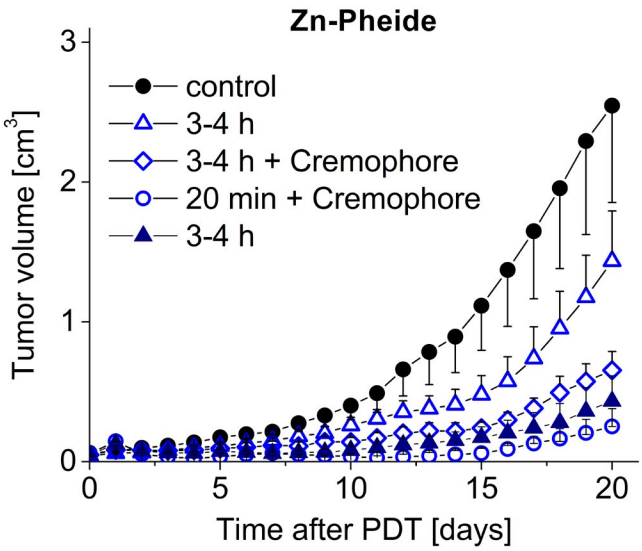

Figure 5: Kinetics of S91 tumors growth after PDT with Zn–Pheide based on different protocols with various irradiation times, doses and ways of administration. Full triangles - 10 mg/kg i.p., empty symbols - 2 mg/kg i.v. (see the text for details). Bars indicate the variance of tumor volumes which increases with the tumor size.

increases to reach a maximum within 0.5-3.5 h, depending on the route of administration and the carrier, followed by a gradual decrease. These changes reflect the initial penetration of the pigment into solid S91 tumors and then its relatively rapid removal. These results confirm the feasibility of obtaining valuable pharmacokinetic data based on *in vivo* emission measurements using fiber optic technology. The technique allows for the detection of a photosensitizer in a subcutaneous tumor with a resolution high enough to distinguish emission signals from two closely-related photosensitizers. Similar results were obtained after intragastric administration of photosensitizers at a dose of 10 mg/kg (data not shown). These characteristic emission signals have never been seen in the tumors of untreated animals, confirming the specificity of the method. This is relevant in light of the fact that Chl derivatives are present in animal food but they are effectively effluxed by xenobiotic transporters and their concentration inside the tissue remains below detection level [13].

The pharmacokinetic profiles of Chl derivatives depend on the way they are administered. The penetration of photosensitizers in tumor tissue is slower after i.p. administration, probably because they have to diffuse from the peritoneal cavity into the circulation and only then into the tumor. Interestingly, no such effect was observed with Photofrin II. The route of its administration had no effect on its tissue levels, only affecting the rate of drug removal from the organism [22].

The solubilization of the photosensitizers in Cremophore® [23,24] brings about a significant increase in pigment concentration in the tumor and a shortening of the time needed to reach the maximum level. In particular, i.v. administration of photosensitizers at a lower dose (2 mg/kg) with a surfactant leads to comparable or even higher drug concentrations in tumors than when a much higher dose of 10 mg/kg is administered i.p. but without the surfactant. This result suggests that very high doses of i.p. administered photosensitizer can be replaced by substantially lower doses administered i.v. with the use of surfactant. The enhancement of cellular uptake due to the surfactant was also observed with 5-aminolevulinic (ALA). For instance, the use of the non-ionic surfactants Tween 80 and pluronic F68 increased the accumulation of ALA in HuCC-T1 cells by 60% [25].

Optimization of PDT protocol

Based on the pharmacokinetic profiles of photosensitizers in tumors, as determined by measuring their fluorescence *in vivo*, PDT with the use of Zn–Pheide was performed according to four protocols (see Scheme 1 and Table 1). The comparison of three low-dose protocols (2 mg/kg, i.v.) showed a clear correlation between the PDT effect and the level of the photosensitizer in tumors during irradiation. The highest efficacy was achieved when a surfactant-solubilized photosensitizer was administered, followed by irradiation after 20 min, which match the onset of the peak level of the photosensitizer in the tumors. Much weaker effects were seen when the photosensitizer was solubilized but the tumors were only irradiated after 3-4 hours and yet weaker when no surfactant was applied.

The optimization of the low-dose protocol by shifting the irradiation to 20 min after i.v. photosensitizer administration, which corresponds to the maximum level of the drug in tumors, gives a response to PDT at least as effective as in the high-dose protocol (10 mg/kg, without the surfactant, i.p., irradiation after 3-4 h). Similar responses to PDT after performing two varied schemes of treatment (different dose of drug, carrier, way of injection and start of irradiation after drug administration) correlated with an almost equal mean photosensitizer level during irradiation. This notion shows that a high dose of Zn–Pheide (10 mg/kg) i.p. administered can be replaced by a much lower dose of 2 mg/kg given i.v. when using a surfactant carrier.

The pharmacokinetics of Chl-derivatives shows their potential advantages over other photosensitizers, both in peak level and retention time in tumors. By comparison, Foscan and hypericin reach a maximal concentration in tumor 24 h after administration [26,27]. Photofrin or Photochlor, in turn, remain in the body up to 3 months after administration, which implies a long period of light sensitivity-related discomfort to patients [28]. Another drug, Tookad (Pd-bacteriopheophorbide), closely related to Chlide and Zn–Pheide, unlike these two pigments does not accumulate in the tumor, but remains in the bloodstream, which allows antivascular targeted PDT. Tookad reaches maximal concentration in plasma 5 minutes after

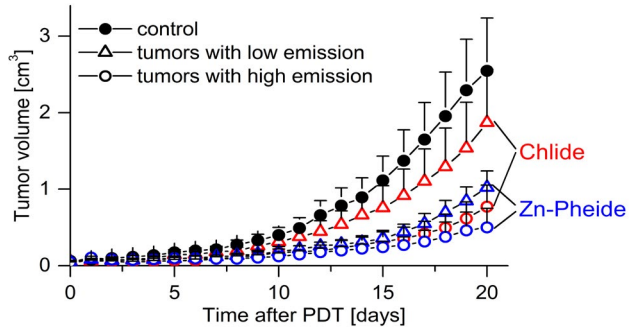

Figure 6: Correlation of the kinetics of S91 tumors growth after PDT with the intensity of photosensitizer fluorescence in the tumors before irradiation. The tumors were divided into two groups using the mean value of the signal intensity (i.e. 52 a.u.), measured just prior irradiation. Control tumors grew in the animals not treated with photosensitizer. Bars indicate the variance of tumor volumes which increases with the tumor size.

injection and then it is rapidly cleared out from plasma, reaching background level within 3 hours [29].

Conclusions and Perspectives

There is a strong correlation between pharmacokinetic profiles and PDT efficacy in mouse model tumors. This confirms the applicability of the fiber-optic based technique of emission detection for real-time *in vivo* monitoring of photosensitizer level. Moreover, considering the spectral properties of human tissue, this technique can be applied in humans, also to internal organs, if combined with endoscopy/laparoscopic surgery to introduce the fiber-optics. Obviously, one of its limitations is the necessity to use fluorescent drugs but this is well compensated for by the many advantages of using this technique. Its potential applications are wide and they extend beyond the use in PDT. For instance, such non-invasive measurements of drug level could be a step toward personalized therapy in humans. Also, it opens a possibility to estimate the activity of xenobiotic transport system on individual basis. In terms of PDT, in particular, it allows for: (1) a maximization of therapeutic effects by indicating the optimal timing for irradiation; (2) a determination of the photosensitizer signal in the tumor in order to predict the response to the therapy; (3) a precise estimation of the safety dark period for the patient to minimize the dangerous side effects of cutaneous phototoxicity; (4) performing a whole series of non-invasive pharmacokinetic experiments in the same organism, in combination with the evaluation of various additional factors (inhibitors, other therapeutics, etc.); and (5) a significant cut in the costs of pharmacokinetic studies.

Acknowledgements

This work was supported by the grant from Foundation for Polish Science (TEAM/2010-5/3 to LF), a grant from the Polish Ministry of Science and Higher Education (0505/B/P01/2011/40 to KU) and a grant from Faculty of Biochemistry, Biophysics and Biotechnology of the Jagiellonian University (WRBW/UJ/2010 to MS). The Faculty is a beneficiary of the structural funds from the European Union, grant No.: POIG.02.01.00-12-064/08 Molecular Biotechnology for Health.

References

1. Wagnières GA, Star WM, Wilson BC (1998) In vivo fluorescence spectroscopy and imaging for oncological applications. Photochem Photobiol 68: 603-632.
2. Fischer F, Dickson EF, Pottier RH, Wieland H (2001) An affordable, portable fluorescence imaging device for skin lesion detection using a dual wavelength approach for image contrast enhancement and aminolaevulinic acid-induced protoporphyrin IX. Part I. Design, spectral and spatial characteristics. Lasers Med Sci 16: 199-206.
3. Anderson RR, Parrish JA (1981) The optics of human skin. J Invest Dermatol 77: 13-19.
4. Braichotte DR, Savary J-F, Monnier P, van den Bergh HE (1996) Optimizing light dosimetry in photodynamic therapy of early stage carcinomas of the esophagus using fluorescence spectroscopy. Laser Surg Med 19: 340-346.
5. Andersson-Engels S, Klinteberg C, Svanberg K, Svanberg S (1997) In vivo fluorescence imaging for tissue diagnostics. Phys Med Biol 42: 815-824.
6. Bigio IJ, Mourant JR (1997) Ultraviolet and visible spectroscopies for tissue diagnostics: fluorescence spectroscopy and elastic-scattering spectroscopy. Phys Med Biol 42: 803-814.
7. Mehta AD, Jung JC, Flusberg BA, Schnitzer MJ (2004) Fiber optic in vivo imaging in the mammalian nervous system. Curr Opin Neurobiol 14: 617-628.
8. Flusberg BA, Cocker ED, Piyawattanametha W, Jung JC, Cheung EL, et al. (2005) Fiber-optic fluorescence imaging. Nat Methods 2: 941-950.
9. Hyde DE, Farrell TJ, Patterson MS, Wilson BC (2001) A diffusion theory model of spatially resolved fluorescence from depth-dependent fluorophore concentrations. Phys Med Biol 46: 369-383.
10. Sevick-Muraca EM, Houston JP, Gurfinkel M (2002) Fluorescence-enhanced, near infrared diagnostic imaging with contrast agents. Curr Opin Chem Biol 6: 642-650.
11. Rosenbach-Belkin V, Chen L, Fiedor L, Tregub I, Pavlotsky F, et al. (1996) Serine conjugates of chlorophyll and bacteriochlorophyll: Photocytotoxicity *in vitro* and tissue distribution in mice bearing melanoma tumors. Photochem Photobiol 65: 174-181.
12. Troy T, Jekic-McMullen D, Sambucetti L, Rice B (2004) Quantitative comparison of the sensitivity of detection of fluorescent and bioluminescent reporters in animal models. Mol Imaging 3: 9-23.
13. Szczygieł M, Urbańska K, Jurecka P, Stawoska I, Stochel G, et al. (2008) Central metal determines pharmacokinetics of chlorophyll-derived xenobiotics. J Med Chem 51: 4412-4418.
14. Jakubowska M, Szczygieł M, Michalczyk-Wetula D, Susz A, Stochel G, et al. (2013) Zinc-pheophorbide a-highly efficient low-cost photosensitizer against human adenocarcinoma in cellular and animal models. Photodiagnosis Photodyn Ther 10: 266-277.
15. Fiedor L, Rosenbach-Belkin V, Sai M, Scherz A (1996) Preparation of tetrapyrrole-amino acid covalent complexes. Plant Physiol Biochem 34: 393-398.
16. Nowak P, Michalik M, Fiedor L, Wozniakiewicz M, Koscielniak P (2013) Capillary electrophoresis as a tool for a cost-effective assessment of the activity of plant membrane enzyme chlorophyllase. Electrophoresis 34: 3341-3344.
17. Drzewiecka-Matuszek A, Skalna A, Karocki A, Stochel G, Fiedor L (2005) Effects of heavy central metal on the ground and excited states of chlorophyll. J Biol Inorg Chem 10: 453-462.
18. Juzeniene A, Juzenas P, Iani V, Moan J (2002) Topical application of 5-aminolevulinic acid and its methylester, hexylester and octylester derivatives: considerations for dosimetry in mouse skin model. Photochem Photobiol 76: 329-334.
19. Amelink A, Sterenborg HJ, Bard MP, Burgers SA (2004) In vivo measurement of the local optical properties of tissue by use of differential path-length spectroscopy. Opt Lett 29: 1087-1089.
20. Chen J, Zhuo S, Luo T, Jiang X, Zhao J (2006) Spectral characteristics of autofluorescence and second harmonic generation from ex vivo human skin induced by femtosecond laser and visible lasers. Scanning 28: 319-326.
21. Zhuo S, Zhu X, Chen J, Xie S (2013) Quantitative biomarkers of human skin photoaging based on intrinsic second harmonic generation signal. Scanning 35: 273-276.
22. Perry RR, Smith PD, Evans S, Pass HI (1991) Intravenous vs intraperitoneal sensitizer: implications for intraperitoneal photodynamic therapy. Photochem Photobiol 53: 335-340.
23. Sparreboom A, van Tellingen O, Nooijen WJ, Beijnen JH (1996) Nonlinear pharmacokinetics of paclitaxel in mice results from the pharmaceutical vehicle Cremophor EL. Cancer Res 56: 2112-2115.
24. Gelderblom H, Verweij J, Nooter K, Sparreboom A (2001) Cremophor EL: the drawbacks and advantages of vehicle selection for drug formulation. Eur J Cancer 37: 1590-1598.

25. Chung CW, Kim CH, Choi KH, Yoo JJ, Kim do H, et al. (2012) Effect of surfactant on 5-aminolevulinic acid uptake and PpIX generation in human cholangiocarcinoma cell. Eur J Pharm Biopharm 80: 453-458.

26. Jones HJ, Vernon DI, Brown SB (2003) Photodynamic therapy effect of m-THPC (Foscan) in vivo: correlation with pharmacokinetics. Br J Cancer 89: 398-404.

27. Uzdensky A, Iani V, Ma LW, Moan J (2006) On hypericin application in fluorescence diagnosis and cancer treatment: pharmacokinetics and photosensitizing efficiency in nude mice bearing WiDr carcinoma. Med Laser Appl 21: 271-276.

28. Bellnier DA, Greco WR, Loewen GM, Nava H, Oseroff AR, et al. (2006) Clinical pharmacokinetics of the PDT photosensitizers porfimer sodium (Photofrin), 2-[1-hexyloxyethyl]-2-devinyl pyropheophorbide-a (Photochlor) and 5-ALA-induced protoporphyrin IX. Lasers Surg Med 38: 439-444.

29. Brun PH, DeGroot JL, Gudgin Dickson EF, Farahani M, Pottier RH (2004) Determination of the *in vivo* pharmacokinetics of palladium-bacteriopheophorbide (WST09) in EMT6 tumour-bearing balb/c mice using graphite furnace atomic absorption spectroscopy. Photochem Photobiol Sci 3: 1006-1010.